



1

2 **Effects of intensified freeze-thaw frequency on dynamics of winter**
3 **nitrogen resources in temperate grasslands**

4 **Chaoxue Zhang^{1,2}, Na Li³, Linna Ma^{1,2,*}**

5 ¹ State Key Laboratory of Forage Breeding-by-Design and Utilization, Institute of
6 Botany, the Chinese Academy of Sciences, Beijing 100093, China
7 ²Key Laboratory of Vegetation and Environmental Change, Institute of Botany, the
8 Chinese Academy of Sciences, Beijing 100093, China
9 ³ Ministry of Education Key Laboratory of Ecology and Resource Use of the
10 Mongolian Plateau, School of Ecology and Environment, Inner Mongolia University,
11 Hohhot 010021, China

12 ***Corresponding author:**
13 Email: maln@ibcas.ac.cn; Tel: +86-10-62836564

14
15
16
17



18 **Abstract**

19 In seasonal snow-covered temperate regions, winter serves as a crucial phase for
20 nitrogen (N) accumulation through persistent mineralization processes. Climate
21 warming has accelerated snowmelt and intensified freeze-thaw cycle frequency (FTC),
22 potentially altering the availability of winter N sources for plants. We simulated
23 intensified FTC regimes (increased 0, 6, and 12 cycles) in situ across two contrasting
24 temperate grasslands, employing dual-labeled isotopes ($^{15}\text{NH}_4^{15}\text{NO}_3$) to quantify
25 winter N dynamics. Our results showed that intensified FTC significantly enhanced
26 soil net ammonification rates and inorganic N levels in early spring, while net
27 nitrification rates remained stable. This suggests that frequent FTC may provide a
28 substantial N source for soil microorganisms and plant growth. Notably, soil microbial
29 biomass N increased despite microbial C limitation, indicating efficient microbial N
30 competition that restricted plant access to winter N sources. Intensified low-frequency
31 FTC did not affect plant ^{15}N acquisition, whereas high-frequency FTC significantly
32 reduced plant ^{15}N acquisition. Importantly, the impacts of FTC on plant ^{15}N
33 acquisition varied among functional types. Dominant cold-tolerant species (perennial
34 bunch grasses and semi-shrubs) increased ^{15}N acquisition, likely due to earlier root
35 activity, while subordinate species (perennial rhizome grasses and forbs) exhibited
36 reduced acquisition. In conclusion, while intensified FTC did not lead to the loss of
37 winter N sources, it restructures N availability by favoring microbial retention and
38 creating competitive hierarchies among plants in temperate grasslands. The
39 high-frequency FTC-induced shifts in partitioning of winter N resources could



40 substantially influence grassland productivity and community structure, highlighting

41 the critical need to integrate winter climate change effects into temperate grassland

42 ecosystem models.

43 **Keywords:** freeze-thaw cycle; grassland; N isotope; N dynamic; plant N acquisition;

44 snowmelt; winter



1 Introduction

Approximately 50 % of terrestrial ecosystems in the Northern Hemisphere experience seasonal snow cover and winter soil freezing (Sommerfeld et al., 1993; IPCC, 2021). Remarkably, soil microorganisms maintain metabolic activity under snowpack and contribute to nutrient mineralization throughout winter (Larsen et al., 2012; Zhang et al., 2011). These winter processes, including soil nitrogen (N) mineralization and microbial N immobilization, constitute a vital nutrient reservoir that supports plant growth across alpine grasslands, temperate grasslands, and boreal forests (Alatalo et al., 2014; Bilbrough et al., 2000; Collins et al., 2017; Edwards and Jefferies, 2010). The springtime release of winter-accumulated N (mainly including NH_4^+ , NO_3^- , and dissolved organic N) through freeze-thaw cycles (FTC) synchronizes nutrient availability with plant demand (Kaiser et al., 2011), particularly in N-limited ecosystems where winter N contributions may determine growing season productivity (Schmidt and Lipson, 2004).

Climate warming has emerged as one of the most important global environmental challenges. Evidence shows that climate warming has primarily occurred during winter, with the rate of winter warming exceeding the annual average over the past few decades in China (Zong and Shi, 2020). This trend is expected to intensify, with an anticipated increase in the frequency of extreme warming events (Kreyling et al., 2011; IPCC, 2021). Winter warming might lead to an earlier onset and intensified frequency of freeze-thaw cycles (FTC), potentially altering ecosystem N cycling



23 processes (Gao et al., 2018). Consequently, this could affect the availability of winter
24 N sources for plant growth. However, how intensified FTC affect winter N retention
25 remains poorly understood, particularly its subsequent impacts on plant N uptake and
26 ecosystem functioning.

27

28 Intensified FTC induces complex shifts in soil N dynamics by simultaneously
29 enhancing N mineralization while disrupting microbial immobilization and ecosystem
30 retention processes. Existing research have demonstrated that intensified FTC can
31 enhance soil N availability in cold regions (Dai et al., 2020; Nie et al., 2024; Teepe
32 and Ludwig, 2004; Wang et al., 2012; Yang et al., 2023). The physical disruption
33 caused by FTC promotes the N release from both soil organic matter and microbial
34 biomass via cell lysis (Koponen et al., 2006; Sawicka et al., 2010; Skogland et al.,
35 1988). However, this FTC-induced N pulse often occurs before plants resume active
36 uptake, leading to substantial N losses through leaching and gaseous emissions (Chen
37 et al., 2021; Elrys et al., 2021; Ji et al., 2024). while microbial mortality reduces
38 microbial N immobilization (Gao et al., 2018), the surviving microbial community
39 exhibits stimulated microbial activity that accelerates nutrient cycling (Fitzhugh et al.,
40 2001; Nie et al., 2024; Sharma et al., 2006; Wang et al., 2024). Notably, a
41 comprehensive meta-analysis by Song et al. (2017) indicated that FTC have no
42 significant effect on microbial biomass N (MBN) across various ecosystems,
43 including forest, shrubland, grassland/meadow, cropland, tundra and wetland
44 ecosystems, suggesting complex compensatory mechanisms in microbial N retention.



45

46 Frequent FTC significantly impact plant-soil N dynamics through multiple pathways.
47 Root damage caused by FTC directly impairs plant N acquisition capacity (Campbell
48 et al., 2014; Song et al., 2017), while simultaneously creating temporal mismatches in
49 N availability. Larsen et al. (2012) utilized ^{15}N tracer reveals that soil microorganisms
50 initially dominate winter N immobilization following snowmelt, with plant functional
51 types exhibiting sequential N uptake patterns: evergreen dwarf shrubs being the first
52 to take up winter N, succeeded by deciduous dwarf shrubs and graminoids in late
53 spring in the alpine ecosystem. This study highlighted a temporal differentiation in the
54 resumption of N uptake among plant functional groups after winter. This temporal
55 niche partitioning is particularly pronounced in temperate regions, where shallower
56 snowpack and more frequent spring FTC create distinct competitive environments
57 compared to alpine systems. Studies in temperate grasslands have shown that
58 perennial bunch grasses present earlier N uptake than perennial rhizome grasses and
59 forbs (Ma et al., 2018, 2020), a phenological advantage that becomes more
60 pronounced under winter warming conditions (Turner and Henry, 2009). These
61 findings collectively highlight how FTC-mediated changes in belowground processes
62 interact with plant functional traits to govern winter N partitioning.

63

64 While previous studies have examined winter N cycling in high-altitude and
65 high-latitude regions experiencing rapid warming trends (Alatalo et al., 2014;
66 Bilbrough et al., 2000; Brooks et al., 1996; Edwards and Jefferies, 2010; Miller et al.,



2007), temperate grasslands remain understudied despite their distinct freeze-thaw regimes. Critically, existing research has predominantly relied on laboratory simulations employing artificial freezing regimes (DeLuca et al., 1992; Teepe and Ludwig, 2004; Yang et al., 2023; Zhang et al., 2024), creating significant gaps regarding the ecological impacts of natural in situ freeze-thaw cycles. Field-based investigations are urgently needed to address two critical questions: (1) how FTC frequency alters winter N retention dynamics, and (2) whether these changes create legacy effects on subsequent growing season productivity and plant community composition in temperate grasslands. This lack of field evidence limits our ability to predict ecosystem responses to climate change.

Temperate grasslands cover nearly 40 % of China's terrestrial ecosystems (Bardgett et al., 2021), and are particularly vulnerable to climate change due to their prolonged near-freezing winter conditions. To understand how intensified FTC affect retention of winter N resources in grasslands, we conducted an in situ $^{15}\text{NH}_4^{15}\text{NO}_3$ tracer experiment across two temperate grassland types. We hypothesize that: (1) intensified FTC would reduce retention of winter N resources through physical disruption of soil aggregates enhancing N mobility, root damage impairing plant N uptake capacity, and microbial cell lysis leading to N leaching and denitrification losses (Fitzhugh et al., 2001; Koponen et al., 2006; Nie et al., 2024; Sawicka et al., 2010; Sharma et al., 2006; Skogland et al., 1988); and (2) intensified FTC would lead to differential utilization of winter N sources among plant species, mediated by interspecific variations in their



89 competitive abilities, root system architecture (particularly rooting depth and winter
90 root activity), and temporal niche partitioning in growth phenology (Bilbrough et al.,
91 2000; Hosokawa et al., 2017; Ma et al., 2018, 2020). Specifically, we expected that
92 deep-rooted species with early spring green-up would increase their utilization of
93 winter N sources, while other plants may experience reduced N utilization due to root
94 damage (Campbell et al., 2014; Song et al., 2017).

95

96 **2 Methods**

97 **2.1 Experimental site**

98 We conducted parallel experiments in two contrasting temperate grassland ecosystems:
99 a meadow steppe and a sandy steppe (Table 1; Fig. 1). The meadow steppe was
100 situated at the Hulunber Grassland Ecosystem Observation and Research Station in
101 northeastern China (49°19' N, 120°02' E, 628 m), while the sandy steppe was located
102 at the Ordos Sandy Grassland Ecology Research Station in northern China (39°29' N,
103 110°11' E, 1290 m).

104

105 Both sites have a continental climate. The mean annual precipitation is 420 mm and
106 310 mm, and the mean annual temperature is -2-1 °C and 6.5 °C in the meadow
107 steppe and the sandy steppe, respectively (<http://data.cma.cn/>). The non-growing
108 season for the meadow steppe extends from late September to late April of the
109 following year, with a spring freeze-thaw period occurring from late March to late
110 April. In contrast, the non-growing season for the sandy steppe lasts from



111 mid-October to late March, with the spring freeze-thaw period occurring from late
112 February to late March. In the meadow steppe, persistent snow cover reached 20-25
113 cm depth during late winter (January-February), providing consistent thermal
114 insulation. In contrast, the sandy steppe exhibited shallower and more variable
115 snowpack (typically 10 cm depth) due to higher wind redistribution and lower
116 moisture retention. Under natural conditions, the meadow steppe in this study
117 underwent a total of 19 freeze-thaw cycles, while the sandy steppe experienced 21
118 freeze-thaw cycles in early spring (<http://nm.cma.gov.cn/>).
119
120 The meadow steppe features high plant diversity and fertile soils, while the sandy
121 steppe exhibits lower diversity and nutrient-poor, coarse-textured soils (Table 1). This
122 strategic pairing allows for comprehensive assessment of FTC impacts across varying
123 resource availability and community structures, as evidenced by significant baseline
124 differences in N dynamics between sites. According to the Chinese Soil Classification
125 (GB/T 17296-2009), the predominant soil type in meadow grassland is loam soil, and
126 which in sandy grassland is sandy loam soil. The meadow steppe soil has higher C
127 and N content but slightly lower pH compared to the sandy steppe soil (Table 1). In
128 the meadow steppe, the dominant plant species include perennial bunch grasses like
129 *Stipa baicalensis* Roshev, perennial rhizome grasses such as *Leymus chinensis* (Trin.)
130 Tzvel., as well as perennial forbs including *Carex pediformis* C. A. Mey., which
131 together cover approximately 78% of the site. In the sandy steppe, the dominant plant
132 species are *Cleistogenes squarrosa* (Trin.) Keng., *Klasea centauroides* (L.) Cass., and



133 *Hedysarum mongolicum* Turez, covering about 70 % of the area (Table 1). The
134 complementary strengths of these ecosystems enable robust predictions about
135 grassland responses to changing winter climate regimes.

136

137 **2.2 Experimental design**

138 In late October 2020, eighteen 3 m × 3 m plots were established at each site, with a
139 3-meter buffer between neighboring plots. The experiment employed a randomized
140 block design with three treatments and six replicates per site: (1) control (ambient
141 FTC), (2) intensified low-frequency FTC (LFTC; + 6 times), and (3) intensified
142 high-frequency FTC (HFTC; + 12 times). These treatments were designed to simulate
143 projected increases in winter FTC frequency under climate change scenarios.

144

145 The treatment levels were based on historical climate data showing approximately 20
146 natural FTCs typically occur during winter and early spring at both sites (Table 1;
147 <https://data.cma.cn/>). According to the definition of freeze-thaw cycling, a
148 freeze-thaw cycle is defined as the process in which soil temperature (0-10 cm) rises
149 above 0 °C and then subsequent drops below 0 °C (Yanai et al., 2007). Therefore, the
150 intensified FTC correspond to total increases in 30 % (+ 6 times) and 60 % (+ 12
151 times) in the frequency of FTC during winter and spring seasons, respectively.

152

153 Within each plot, we established a fixed 1 m × 1 m subplot for ¹⁵N tracing. Building
154 upon established ¹⁵N tracing approaches (Ma et al. 2020; Bilbrough et al. 2000), we



155 applied $^{15}\text{NH}_4^{15}\text{NO}_3$ solution prior to winter soil freezing. A solution containing 24 mg
156 $^{15}\text{N L}^{-1}$ of $^{15}\text{NH}_4^{15}\text{NO}_3$ was injected into 100 holes with a syringe guided by a grid
157 frame (1 m \times 1 m), with each hole receiving 2 mL of the labeled solution. The total
158 application per subplot was 200 mL, which is equal to 120 mg $^{15}\text{N m}^{-2}$. The added ^{15}N
159 was kept within the natural fluctuation range of inorganic N in the soil, approximately
160 7 %-10 % of background soil inorganic N levels. We injected water into control
161 treatments instead of the ^{15}N tracer, and no significant differences in plant/microbial N
162 concentrations when compared to the ^{15}N treatments. This indicates that the ^{15}N
163 application did not disrupt natural N cycling processes (Ma et al., 2018).

164

165 Based on recent 5-year climatic records, our initial FTC treatments were scheduled
166 approximately 15 days prior to the natural spring FTC period (late winter). For the
167 freezing-thaw manipulation, a closed-top tent (3 m length \times 3 m width \times 2 m
168 height) was installed in each plot during each warming manipulation. The heating
169 tents were constructed with polyester fabric, featuring sealed tops and mesh-sided
170 windows to prevent excessive CO_2 accumulation while maintaining temperature
171 control. Within each tent, we used a propane AirHeater (Mr Heater, USA) to raise soil
172 temperature to 2-3 $^{\circ}\text{C}$ (0-15cm), maintaining this temperature continuously for 8 to
173 10 hours each time. Continuous temperature logging was performed using 2
174 temperature detectors per treatment positioned at two critical positions: (a) 5 cm
175 above soil surface (ambient microclimate) and (b) 10 cm soil depth, with data
176 recorded at half-hour intervals throughout the experiment. The temperature was then



177 allowed to drop to approximately -2°C over a period of 4 hours to complete one
178 freeze-thaw cycle. Two intensified FTC regimes were implemented: (i)
179 high-frequency FTC (HFTC) with 12 additional cycles administered every 1-3 days,
180 and (ii) low-frequency FTC (LFTC) with 6 additional cycles every 3-6 days. During
181 the natural freeze-thaw period, all artificial FTC treatments were deliberately
182 conducted when daily mean temperatures remained below -2°C to avoid interference
183 with natural cycles.

184

185 **2.3 Sampling and Processing**

186 Samplings were conducted after the freeze-thaw treatments and during the succeeding
187 growing season. In the meadow steppe, samplings were collected on the following
188 dates: 26 March 2021 (early spring); 4 May 2021 (late spring); 23 June 2021 (early
189 summer); 22 July 2021 (late summer); and 26 September 2021 (late autumn).
190 Similarly, in the sandy steppe, samplings were collected on 5 March 2021 (early
191 spring); 29 April 2021 (late spring); 21 June 2021 (early summer); 26 July 2021 (late
192 summer); and 15 October 2021 (late autumn).

193

194 For plant samplings, soil blocks (20 cm length \times 20 cm width \times 20 cm height)
195 containing dominant plant species were carefully excavated and sectioned. Plant roots
196 were washed with distilled water to remove surface ^{15}N , then separated into
197 aboveground and belowground components. All plant materials were oven-dried at
198 65°C for 48 hours. For soil samplings, we randomly excavated three labeled core at



199 20 cm depth soil (diameter is 3.5 cm) from each plot. We combined three soil core
200 into a composite sample, which was passed through a 2 mm sieve. Within 4 hours of
201 collection, the composite sample was separated into two portions: one for air-drying
202 and soil analysis, and the other stored at -20 °C for microbial analysis.
203
204 Soil temperature and moisture at a depth of 10 cm were measured automatically every
205 half hour using HOBO data loggers (H21-USB, Onset Inc., USA) throughout the
206 study period. Soil and plant (aboveground and belowground) dry samples were
207 pulverized using a ball mill. Subsequently, soil samples were sieved through a
208 100-mesh sieve and plant samples through an 80-mesh sieve. The sieved samples
209 were analyzed for C and N content using an elemental analyzer (Elementar Vario Max
210 CN, Germany). Soil net ammonification and nitrification rates were analyzed using
211 the method of polyvinyl chloride plastic (PVC) core (Raison et al., 1987). A pair of
212 PVC cores was vertically inserted to 20 cm depth soil layer in each plot to incubate
213 the soil without plant uptake. One core was collected as the initial (unincubated)
214 sample to determine the concentrations of $\text{NH}_4^+\text{-N}$ and $\text{NO}_3^-\text{-N}$ using a flow injection
215 autoanalyzer (Scalar SANplus segmented flow analyzer, Netherlands). The other core
216 was incubated in situ for two weeks within capped cores. After incubation, we
217 analyzed the $\text{NH}_4^+\text{-N}$ and $\text{NO}_3^-\text{-N}$ in these samples as well. Net ammonification and
218 nitrification rates were estimated based on the changes in $\text{NH}_4^+\text{-N}$ and $\text{NO}_3^-\text{-N}$ levels
219 between the incubated and initial values. Soil total dissolved organic N (DON) was
220 calculated as total N minus inorganic N (i.e., the sum of $\text{NH}_4^+\text{-N}$ and $\text{NO}_3^-\text{-N}$). Soil



221 total dissolved organic C (DOC) was calculated as total C minus inorganic C.

222

223 The microbial biomass C and N were assessed by the fumigation-extraction

224 method with a total organic C analyzer (TOC multiN/C 3100, Analytik Jena, Germany;

225 Vance et al., 1987). The method calculates microbial biomass C and N by determining

226 the contrast in extractable C or N levels between samples that have been fumigated

227 and those that have not. To prepare the soil extracts, fresh soil samples are moistened

228 to a water retention capacity of 60 %, followed by incubation in the dark at a

229 temperature of 25 °C for a week. After incubation, samples with a moisture content

230 equivalent to 25 g of dry weight were fumigated with chloroform (CHCl₃) for a

231 duration of 24 hours. The soil sample was extracted by agitating it with shaking 60ml

232 K₂SO₄ solution for 30min. After filtration, the extractable concentration of organic C

233 or N was determined by elemental analyzer (Elementar Analyzer, Vario MaxCN,

234 Germany). The conversion coefficient is 0.45. The ¹⁵N contents in plant (2 mg) and

235 soil subsamples (20 mg) were analyzed with an elemental analyzer coupled with an

236 isotope-ratio mass spectrometer (IRMS, Thermo Finnigan MAT DELTAplus XP,

237 USA). Soil microbial ¹⁵N was measured using alkaline persulfate oxidation, followed

238 by a modified diffusion method (Stark and Hart, 1996; Zhou et al., 2003). Soil

239 immobilized ¹⁵N was then calculated by subtracting microbial ¹⁵N from soil total ¹⁵N

240 (Ma et al., 2018).

241

242 Soil microbial community structure was determined using the phospholipid fatty acid



(PLFA) method (Bossio and Scow, 1998). Changes in PLFAs reflect the viable biomass of fungi and bacteria, as well as microbial community structure in situ soils. The fatty acids a13:0, i14:0, i15:0, i16:0, i17:0, a17:0, 16:1 ω 7c, 17:1 ω 8c, 18:1 ω 5c, 18:1 ω 9t, 17:0cy, and 19:0cy were chosen as representative of the bacterial group. The fatty acids 16:1 ω 5c, 18:2 ω 6,9c, and 18:1 ω 9c were selected to represent the fungal group.

249

2.4 Statistical Analysis

The ^{15}N acquisition (% of applied ^{15}N) in the shoot and root were calculated as: $[(^{15}\text{N}_\text{I} - ^{15}\text{N}_\text{a}) \times \text{biomass} / ^{15}\text{N}_\text{t}] \times 100$, where $^{15}\text{N}_\text{I}$ and $^{15}\text{N}_\text{a}$ are the ^{15}N concentrations ($\text{g}^{15}\text{N g}^{-1}$ sample) in the labeled and the control samples; biomass is the shoot or root biomass at each sampling time (g m^{-2}), and $^{15}\text{N}_\text{t}$ is the amount of total added ^{15}N tracer ($\text{g}^{15}\text{N m}^{-2}$).

256

The soil or microbial biomass ^{15}N recovery (% of applied ^{15}N) was calculated as: $[(^{15}\text{N}_\text{I} - ^{15}\text{N}_\text{a}) \times V \times \text{BD} / ^{15}\text{N}_\text{t}] \times 100$, where V represents the soil volume of the 20 cm soil profile ($\text{cm}^3 \text{m}^{-2}$), and BD is the bulk density (g cm^{-3}). Differences in soil, microbial and plant properties, and ^{15}N tracer retention in plants, soil, and microorganisms between the two grasslands were analyzed using One-way ANOVA. Repeated measurement ANOVA was used to analyze the influences of different FTC treatments, sampling times, and grassland types on the measured indicators. Spearman correlation coefficients between variables were calculated using “rcorr”. To assess the



relative importance of predictors for plant ^{15}N acquisition capacity, a random forest model was constructed using the randomForest and rfPermute packages. Model training utilized 70 % of the dataset for parameter optimization, with the remaining 30 % reserved for model validation. All above mentioned analysis were conducted with SPSS 21.0 software (SPSS for Windows, Chicago, IL, USA) and RStudio 2025.05.0 (Posit Software, Boston, MA, USA), and graphics were plotted using SigmaPlot, 14.0, Origin 14.0 and R Studio.

3 Results

3.1 Soil microclimate

The edaphic conditions, including soil total C content, inorganic N content, and texture, exhibited significant differences between the two temperate grasslands ($p < 0.05$; Table 1). Throughout the winter freezing period, the lowest soil temperatures (0–10cm) were about $-23\text{ }^{\circ}\text{C}$ in the meadow steppe and $-20\text{ }^{\circ}\text{C}$ in the sandy steppe, respectively (Fig. 2a, b). In early spring, soil temperatures rose rapidly, accompanied by significant snowmelt. Intensified low-frequency FTCs (LFTC) and high-frequency FTCs (HFTC) enhanced soil moisture by $0.03\text{ m}^3\text{ m}^{-3}$ and $0.05\text{ m}^3\text{ m}^{-3}$, respectively, and raised soil temperatures by $2\text{ }^{\circ}\text{C}$ and $3\text{ }^{\circ}\text{C}$ during the period. However, neither intensified LFTC nor HFTC had any significant impact on soil moisture or temperature in the subsequent growing season (Fig. 2a, b).

3.2 Soil characteristics



287 Throughout the study period, intensified LFTC and HFTC only significantly
288 increased soil NH_4^+ -N levels in spring, but did not show any significant effects in the
289 following season ($p < 0.05$, Fig. 3a, b). In the meadow steppe, intensified LFTC and
290 HFTC significantly increased soil NH_4^+ -N levels by 25.0 % and 24.0 % in late spring,
291 respectively ($p < 0.05$, Fig. 3a). Additionally, intensified LFTC enhanced net
292 ammonification rates by 44.3 % and 58.6 %, and HFTC increased them by 58.3 %
293 and 50.3 % in early and late spring, respectively ($p < 0.05$, Fig. 3e). In the sandy
294 steppe, LFTC and HFTC increased soil NH_4^+ -N by 25.0 % and 23.3 % in late spring
295 ($p < 0.05$, Fig. 3b). Intensified LFTC had no significant impact on net ammonification
296 rates, while HFTC increased net ammonification rates by 16.2 %, 63.3 %, and 37.2 %
297 in early spring, late spring, and early summer, respectively ($p < 0.05$, Fig. 3f). It is
298 important to note that neither LFTC nor HFTC had significant effects on NO_3^- -N or
299 net nitrification rates at either site throughout the study period ($p < 0.05$, Fig. 3c, d, g,
300 h).
301
302 Intensified LFTC significantly decreased the soil microbial biomass C (MBC) in
303 spring, while the effect of HFTC on microbial biomass N (MBN) persisted to summer
304 ($p < 0.05$, Fig. 4a-d). In the meadow steppe, HFTC decreased MBC by 16.2 % ($p <$
305 0.05, Fig. 4a). Conversely, both LFTC and HFTC increased MBN by 26.2 % and
306 26.9 %, respectively ($p < 0.05$, Fig. 4c). In the sandy steppe, HFTC decreased MBC
307 by 11.3% in early spring. Unlike MBC, both LFTC and HFTC increased MBN by
308 8.5 % and 28.2 %, respectively ($p < 0.05$, Fig. 4b, d).



309

310 **3.3 Plant properties**

311 Intensified LFTC did not have significant influences on shoot and root biomass N of
312 the selected plant species during the growing season at either site (Fig. 5a-f). In the
313 meadow steppe, HFTC increased shoot and root biomass N of *Stipa baicalensis*
314 (perennial bunch grass) by 19.7 % and 21.8 % at the end of the growing season,
315 respectively. Conversely, HFTC decreased shoot and root biomass N of *Leymus*
316 *chinensis* (perennial rhizome grass) by 23.9 % and 16.2 %, and decreased those of
317 *Carex pediformis* (perennial forb) by 22.2 % and 18.0 % ($p < 0.05$, Fig. 5a, c, e). In
318 the sandy steppe, HFTC increased the shoot and root biomass N of *Hedysarum*
319 *mongolicum* (semi-shrub) by 22.6 % and 23.7 %, respectively. However, HFTC
320 decreased those of *Cleistogenes squarrosa* (perennial bunch grass) by 25.3 % and
321 12.1 %, and those of *Klasea centauroides* (perennial forb) by 23.1 % and 20.3 %. ($p <$
322 0.05, Fig. 5b, d, f).

323

324 **3.4 ^{15}N Retention in the soil-microorganism-plant systems**

325 In both grassland types, soil ^{15}N recovery was highest in early spring, followed by a
326 rapid decline from late spring to late summer. This was then followed by a gradual
327 increase in recovery until late autumn (Fig. 6c, d). In contrast, plant ^{15}N acquisition
328 increased steadily throughout the growing season in both grasslands, while microbial
329 ^{15}N recovery exhibited only modest fluctuations over the entire growing season ($p <$
330 0.05, Fig. 6e-h).



331

332 During the early growing season, intensified LFTC had no significant effect on total
333 ^{15}N recovery in soil-microorganism-plant systems, while intensified HFTC
334 significantly increased total ^{15}N recovery (Fig. 6a, b). LFTC did not significantly
335 impact soil ^{15}N recovery, but HFTC significantly increased soil ^{15}N recovery in the two
336 grasslands ($p < 0.05$, Fig. 6c, d). In the meadow steppe, intensified LFTC and HFTC
337 significantly enhanced microbial ^{15}N recovery by 38.0% and 26.6%, respectively, and
338 by 49.5 % and 32.5 % in the sandy steppe ($p < 0.05$, Fig. 6e, f). Intensified LFTC did
339 not significantly impact plant ^{15}N acquisition; in contrast, intensified HFTC
340 significantly decreased plant ^{15}N recovery in the two grasslands ($p < 0.05$, Fig. 6g, h).

341

342 In the meadow steppe, the ^{15}N acquisition in the shoots of *Stipa baicalensis* (perennial
343 bunch grass) and *Carex pediformis* (perennial forb) were comparable, while *Leymus*
344 *chinensis* (perennial rhizome grass) exhibited lower ^{15}N acquisition. In contrast, the
345 highest ^{15}N acquisition in roots was observed in *Leymus chinensis*, followed by *Carex*
346 *pediformis* and *Stipa baicalensis*. In the sandy steppe, both shoot and root ^{15}N
347 acquisition of *Hedysarum mongolicum* (semi-shrub) were the highest among the
348 studied species. This was followed by the shoot ^{15}N acquisition of *Cleistogenes*
349 *squarrosa* (perennial bunch grass) and *Klasea centauroides* (perennial forb). Notably,
350 the root ^{15}N acquisition of *Klasea centauroides* was higher than that of *Cleistogenes*
351 *squarrosa*.

352



353 In the meadow steppe, HFTC increased shoot and root ^{15}N acquisition of *Stipa*
354 *baicalensis* by 5.8 % and 9.3 %, respectively. In contrast, HFTC decreased ^{15}N
355 acquisition in *Leymus chinensis* by 16.4 % and 12.1 %, and in *Carex pediformis* by
356 4.9 % and 7.8 % ($p < 0.05$, Fig. 7a, c, e). In the sandy steppe, shoot and root ^{15}N
357 acquisition of *Hedysarum mongolicum* increased by 3.8 % and 18.4 %, respectively.
358 Conversely, *Cleistogenes squarrosa* experienced decreases of 16.7 % in shoots and
359 14.4 % in roots, while *Klasea centauroides* showed the largest reductions, with
360 decreases of 16.1 % and 14.1 % in shoot and root ^{15}N acquisition, respectively ($p <$
361 0.05 , Fig. 7b, d, f).

362

363 **3.5 Controls on plant N acquisition**

364 In meadow steppe, correlation analysis revealed that plant ^{15}N acquisition exhibited
365 the strongest positive correlation with soil temperature, followed by bacterial biomass,
366 soil NO_3^- -N levels, soil moisture, soil DOC and fungal biomass under LFTC ($p < 0.05$,
367 Fig. 8a). Negative correlations between net mineralization rates and plant ^{15}N
368 acquisition were observed. Under HFTC, plant ^{15}N acquisition showed the strongest
369 positive correlation with soil temperature, while bacterial biomass, soil NO_3^- -N levels,
370 soil dissolved organic C, microbial biomass C, and soil moisture also exhibited
371 significant positive correlations. In contrast, net nitrification rate, soil NH_4^+ -N levels,
372 and soil total N content displayed significant negative correlations with plant ^{15}N
373 acquisition ($p < 0.05$, Fig. 8b).

374



375 In sandy steppe, plant ^{15}N acquisition exhibited the strongest positive correlation with
376 soil total C content, followed with microbial biomass N, soil total N content, soil
377 temperature, soil dissolved organic C and N, and soil NO_3^- -N levels Under LFTC ($p <$
378 0.05, Fig. 8c). Conversely, fungal biomass, microbial biomass C, microbial biomass
379 C-to-N ratio, and bacterial biomass demonstrated the most significant negative
380 correlations with plant ^{15}N acquisition ($p < 0.05$, Fig. 8c). Under HFTC, plant ^{15}N
381 acquisition exhibited the strongest positive correlation with soil total N content, while
382 significant positive correlations were also observed with soil total C content, soil
383 temperature, microbial biomass N, soil dissolved organic C and N. In contrast, the
384 microbial C-to-N ratio, and microbial biomass showed significant negative
385 correlations with plant ^{15}N acquisition ($p < 0.05$, Fig. 8d).

386

387 Random forest analysis further identified soil temperature as the primary predictor of
388 plants ^{15}N acquisition capability across all treatments ($p < 0.05$, Fig. 9). In the
389 meadow steppe, dominant predictors shifted from soil total N, bacterial biomass, and
390 net nitrification rate under LFTC to a broader suite of predictors including soil total N,
391 bacterial biomass, soil moisture, soil NH_4^+ -N levels, and soil dissolved organic C
392 content under HFTC ($p < 0.05$, Fig. 9a, b). In the sandy steppe, bacterial biomass,
393 fungal biomass, soil NO_3^- -N levels, and soil total N were key predictors under LFTC,
394 while soil moisture, soil total N, bacterial biomass, net nitrification rate, and net
395 ammonification rate were important predictors under HFTC ($p < 0.05$, Fig. 9c, d).

396



397 **4 Discussion**

398 **4.1 Contrasting FTC sensitivity in temperate grasslands**

399 This study investigated how intensified freeze-thaw cycles (FTC) affect dynamics of
400 winter N sources during subsequent growing seasons in two contrasting temperate
401 grasslands, using a $^{15}\text{NH}_4^{15}\text{NO}_3$ tracer. Contrary to our first hypothesis, intensified
402 FTC significantly enhanced soil net ammonification rates and inorganic N levels,
403 though net nitrification rates remained unaffected (Fig. 3). Our findings are consistent
404 with previous research indicating that intensified FTC significantly enhanced spring
405 soil inorganic N content across diverse ecosystems, including temperate forests,
406 alpine meadows, and wetlands (Dai et al., 2020; Ji et al., 2024; Nie et al., 2024; Teepe
407 and Ludwig, 2004; Wang et al., 2012; Yang et al., 2023). A possible explanation for
408 this phenomenon is that frequent FTC promote the release of DON through the
409 physical disruption of soil aggregates and microbial lysis (Koponen et al., 2006;
410 Sawicka et al., 2010; Skogland et al., 1988). This process likely stimulates microbial
411 activity, accelerating mineralization processes (Fitzhugh et al., 2001; Nie et al., 2024;
412 Sharma et al., 2006). The lack of significant change in NO_3^- levels could be attributed
413 to leaching and minimal variations in nitrification rates (Gao et al., 2018). Notably,
414 substantial retention of soil N and soil microbial biomass N (MBN) (Figure 4, 6)
415 suggests that intensified FTC in early spring did not result in substantial loss of winter
416 N sources, but instead enhanced N availability for plants and soil microbial growth.
417
418 The meadow steppe showed greater sensitivity to FTC than the sandy steppe, with



419 even increased low-frequency FTC enhancing net ammonification rates (Fig. 3).
420 Following spring thaw, the effects of FTC on ammonification rates and ^{15}N retention
421 gradually diminished, suggesting these perturbations primarily create early-season
422 pulses rather than sustained changes. The differential response in the sandy steppe
423 could reflect its coarser texture, lower organic matter content, and more
424 drought-adapted microbial community that may be inherently more resistant to
425 FTC-induced disturbance (Yanai et al., 2007; Lipson et al., 2000). The contrasting
426 sensitivity between the two grasslands highlights the importance of considering
427 ecosystem-specific characteristics when predicting biogeochemical responses to
428 climate change.

429

430 **4.2 Intensified FTC alters microbial nutrient-use strategies**

431 Our study found that intensified FTC significantly reduced soil microbial biomass C
432 (MBC) during the early growing season in both grasslands (Fig. 4), consistent with
433 previous observations of microbial lysis under FTC conditions (DeLuca et al., 1992;
434 Walker et al., 2006). This reduction in MBC is mechanistically connected to DOC
435 loss due to intensified FTC (Deng et al., 2023). During snowmelt, soil DOC pool
436 becomes susceptible to leaching, particularly in early spring when plant uptake is
437 minimal, leading to a transient C limitation that further constrains MBC recovery
438 (Lipson et al., 2000; Sullivan et al., 2020). Interestingly, although significant
439 decreases in MBC were observed, microbial biomass N (MBN) presented significant
440 increases in early spring (Fig. 4). This increase in MBN may be attributed to enhanced



441 ammonification rates, which allows soil microorganisms to luxuriously utilize soil
442 inorganic N (Christopher et al., 2008; Nielsen et al., 2001; Skogland et al., 1988;
443 Wang et al., 2024; Yu et al., 2011). This decoupled response between MBC and MBN
444 suggests that soil microorganisms can effectively compete for winter-accumulated N
445 even when C becomes limiting, highlighting their adaptive capacity to prioritize N
446 storage under environmental stress (Yu et al., 2011). This also indicates that
447 FTC-induced stress triggers shift in microbial stoichiometry to optimize N retention at
448 the expense of C use efficiency (Schimel and Bennett, 2004), underscoring how
449 winter climate change may fundamentally alter microbial nutrient cycling strategies in
450 temperate grasslands.

451

452 **4.3 Limited losses of winter N resources under intensified FTC**

453 Our study reveals that intensified FTC did not cause significant losses of winter N
454 resources in temperate grassland ecosystems. We observed that intensified FTC
455 resulted in an increase in total ^{15}N recovery within soil-microorganism-plant systems
456 during the early growing season, though this effect diminished over time and
457 eventually returned to ambient levels (Fig. 6 a, b), indicating that effective
458 ecosystem-level N retention mechanisms. The observed N retention capacity suggests
459 these ecosystems may be more resistant to winter climate change than previously
460 assumed (Han et al., 2018; Song et al., 2017). First, soil ^{15}N recovery remained
461 significantly elevated throughout the entire growing season following FTC, indicating
462 efficient physical protection and chemical stabilization of released N within the soil



463 pool (Fig. 6). Second, microbial ^{15}N recovery increased during the early growing
464 season after intensified FTC but gradually returned to ambient levels in the
465 mid-growing season (Fig. 6). This dynamic suggests that soil microorganisms rapidly
466 immobilized winter N resources during early spring, then progressively released it to
467 support subsequent plant growth (Bilbrough et al., 2000; Zheng et al., 2024; Turner
468 and Henry, 2009). Furthermore, the temporal decoupling of microbial N
469 immobilization and plant N uptake may serve as an important stabilizing mechanism
470 of winter N resources, preventing competitive exclusion while fostering mutually
471 beneficial plant-microbe interactions (Ma et al. 2020).

472

473 **4.4 Divergent plant strategies for ^{15}N acquisition under intensified FTC**

474 Our findings partially support second hypothesis, revealing that high-frequency FTC
475 significantly reduced overall plant ^{15}N acquisition, with contrasting responses
476 observed among different plant functional types (Fig. 7). While dominant species (*S.*
477 *baicalensis* in the meadow steppe and *H. mongolicum* in the sandy steppe)
478 demonstrated enhanced ^{15}N acquisition under intensified high-frequency FTC, other
479 perennial grasses (*L. chinensis* and *C. squarrosa*) and forbs (*C. pediformis* and *K.*
480 *centauroides*) showed reduced ^{15}N uptake. These effects are likely attributed to
481 phenological differences in N acquisition timing, species-specific root system
482 vulnerability to FTC damage, and variation in competitive abilities under FTC stress
483 (Hosokawa et al., 2017; Reinmann et al., 2019; Song et al., 2017).

484



485 The increased ^{15}N acquisition by dominant species likely reflects their ecological
486 adaptations to cold conditions (Fig. 5). *S.baicalensis*, as a cold-tolerant bunchgrass
487 with early spring phenology (Ma et al., 2018; Wang et al., 2016), and *H.monglicum*,
488 as a deep-rooted legume with nitrogen-fixing capability (Lonati et al., 2015), were
489 able to maintain root activity during freezing periods (Larsen et al., 2012) and
490 effectively compete for winter N sources. This aligns with observations that dominant
491 species can meet N demands during growing seasons through winter root activity
492 (Bilbrough et al., 2000; Miller et al., 2009).

493
494 The decreased ^{15}N acquisition in subordinate species (perennial rhizome grasses and
495 forbs) reflects a complex physiological constraints and ecological trade-offs. Their
496 later N uptake phenology (Ma et al., 2018), coupled with greater susceptibility of fine
497 roots to FTC damage (Campbell et al., 2014; Song et al., 2017), limited their ability to
498 absorb winter N sources. First, the delayed N acquisition phenology of these species
499 creates a critical disadvantage. As demonstrated by Ma et al. (2018), perennial
500 rhizome grasses and forbs initiate ^{15}N uptake significantly later than dominant bunch
501 grasses, particularly following freeze-thaw events, missing the early N pulse.
502 Additionally, intensified HFTC induces substantial fine root damage (Campbell et al.,
503 2014; Song et al., 2017), leading to increase mortality rates and constraining their
504 capacity to access winter N sources (Hosokawa et al., 2017; Reinmann et al., 2019).
505 In this study, the significant reduction in root biomass N supports these mechanistic
506 explanations (Fig. 5).



507

508 Second, although rhizome grasses have substantial coverage, they are less competitive
509 than bunch grasses and are more susceptible to environment disturbances, making
510 them vulnerable to damage during FTC period (Walker et al., 2004). Similarly,
511 perennial forbs (*Carex pediformis*) possess slender and creeping roots, which are also
512 prone to damage from FTC (Ye et al., 2017). These findings highlight intensified
513 HFTC may alter competitive hierarchies in grassland ecosystems by favoring
514 cold-adapted dominant species while disadvantaging other functional groups. Such
515 shifts could have important implications for plant community structure and ecosystem
516 functioning under changing winter climate conditions, particularly through potential
517 changes in N cycling dynamics and species composition.

518

519 **4.5 Future research directions**

520 To advance our understanding of intensified FTC effects on N dynamics in temperate
521 grasslands, future research should prioritize three key directions: first, molecular
522 characterization of cold-adapted microbial communities would elucidate the specific
523 taxa and functional genes responsible for retention of winter N resources during FTC
524 events, providing insights into the microbial mechanisms underpinning ecosystem
525 resilience; second, longer-term studies tracking ^{15}N fate across multiple annual
526 freeze-thaw cycles are needed to assess whether the observed N retention patterns
527 persist over long timescales; finally, comparative investigations across diverse
528 grassland types and climatic gradients would help determine how soil properties,



529 vegetation composition, and regional climate modulate ecosystem responses to winter
530 climate change, enabling more accurate predictions of biogeochemical cycling under
531 future climate scenarios.

532

533 **5 Conclusions**

534 Our study provides novel mechanistic insights into how intensified frequency of
535 freeze-thaw cycles (FTC) regulate the dynamics of winter N sources in temperate
536 grasslands. Three important advanced emerge from our findings: first, the observed
537 decoupling of ammonification and nitrification processes under intensified FTC
538 reveals enhanced retention of winter N resources. Second, the microbial community
539 demonstrates remarkable adaptability to FTC stress, maintaining efficient N
540 immobilization despite carbon limitation, as evidenced by increased microbial
541 biomass N concurrent with decreased biomass C. Most importantly, intensified
542 high-frequency FTC reduced overall plant ^{15}N acquisition, with divergent responses
543 among functional types: dominant cold-tolerant species (perennial bunch grasses and
544 semi-shrubs) maintained higher ^{15}N acquisition through phenological advantages,
545 while subordinate species (perennial rhizome grasses and forbs) showed reduced
546 uptake. These findings indicate that microbial communities serve as resilient buffers
547 against N loss during FTC events, and plant functional traits mediate ecosystem-level
548 responses to changing winter conditions. The demonstrated partitioning patterns of
549 winter N resources challenge current models of grassland N cycling by revealing the
550 importance of winter processes in shaping growing season N availability. Future



551 research should focus on quantifying how these FTC-induced N dynamics scale to
552 influence multi-year ecosystem trajectories under climate change scenarios.

553

554 **Author Contributions.** L.M. and C.Z. conceived the project. C.Z. performed the field
555 experiments. C.Z. contributed datasets. C.Z. and N.L. interpreted the results. L.M. and
556 C.Z. wrote the manuscript.

557

558 **Acknowledgements.** The authors thank the Hulunber Grassland Ecosystem
559 Observation and Research Station, Chinese Academy of Agricultural Sciences and the
560 Ordos Sandy Grassland Ecology Research Station, Chinese Academy of Sciences for
561 help with logistics and access permission to the study site.

562

563 **Financial support.** The authors acknowledge the funding provided by the National
564 Natural Science Foundation of China (No. 32071602).

565

566 **Data availability statement.** All data are included in the manuscript.

567 **Conflict of interest.** The authors declare that they have no conflict of interest.

568

569 References

- 570 Alatalo, J. M., Jägerbrand, A. K., and Molau, U.: Climate change and climatic events:
571 community-, functional- and species-level responses of bryophytes and lichens
572 to constant, stepwise, and pulse experimental warming in an alpine tundra, *Alp.*
573 *Botany.*, 124, 81-91, <https://doi.org/10.1007/s00035-014-0133-z>, 2014.
- 574 Bardgett, R. D., Bullock, J. M., Lavorel, S., Manning, P., Schaffner, U., Ostle, N.,
575 Chomel, M., Durigan, G., L. Fry, E., Johnson, D., Lavalley, J. M., Le Provost,
576 G., Luo, S., Png, K., Sankaran, M., Hou, X., Zhou, H., Ma, L., Ren, W., Li, X.,
577 Ding, Y., Li, Y., and Shi, H.: Combatting global grassland degradation, *Nat.*
578 *Rev. Earth Environ.*, 2, 720-735, <https://doi.org/10.1038/s43017-021-00207-2>,
579 2021.
- 580 Bossio, D., Scow, K.: Impacts of Carbon and Flooding on Soil Microbial
581 Communities: Phospholipid Fatty Acid Profiles and Substrate Utilization
582 Patterns, *Microb. Ecol.*, 35, 265-278, <https://doi.org/10.1007/s002489900082>,
583 1998.
- 584 Bilbrough, C. J., Welker, J. M., and Bowman, W. D.: Early Spring Nitrogen Uptake by
585 Snow-Covered Plants: A Comparison of Arctic and Alpine Plant Function
586 under the Snowpack, *Arct. Antarct. Alp. Res.*, 32, 404-411,
587 <https://doi.org/10.1080/15230430.2000.12003384>, 2000.
- 588 Brooks, P. D., Williams, MarkW., and Schmidt, StevenK.: Microbial activity under



- 589 alpine snowpacks, Niwot Ridge, Colorado, *Biogeochemistry*, 32, 93-113,
590 <https://doi.org/10.1007/BF00000354>, 1996.
- 591 Campbell, J. L., Soggi, A. M., and Templer, P. H.: Increased nitrogen leaching
592 following soil freezing is due to decreased root uptake in a northern hardwood
593 forest, *Global Change Biol.*, 20, 2663-2673, <https://doi.org/10.1111/gcb.12532>,
594 2014.
- 595 Chen, M., Zhu, X., Zhao, C., Yu, P., Abulaizi, M., and Jia, H.: Rapid microbial
596 community evolution in initial *Carex* litter decomposition stages in
597 Bayinbuluk alpine wetland during the freeze-thaw period, *Ecol. Indic.*, 121,
598 107180, <https://doi.org/10.1016/j.ecolind.2020.107180>, 2021.
- 599 Christopher, S. F., Shibata, H., Ozawa, M., Nakagawa, Y., and Mitchell, M. J.: The
600 effect of soil freezing on N cycling: comparison of two headwater
601 subcatchments with different vegetation and snowpack conditions in the
602 northern Hokkaido Island of Japan, *Biogeochemistry*, 88, 15-30,
603 <https://doi.org/10.1007/s10533-008-9189-4>, 2008.
- 604 Collins, S. L., Ladwig, L. M., Petrie, M. D., Jones, S. K., Mulhouse, J. M., Thibault, J.
605 R., and Pockman, W. T.: Press-pulse interactions: effects of warming, N
606 deposition, altered winter precipitation, and fire on desert grassland
607 community structure and dynamics, *Global Change Biol.*, 23, 1095-1108,
608 <https://doi.org/10.1111/gcb.13493>, 2017.
- 609 Dai, Z., Yu, M., Chen, H., Zhao, H., Huang, Y., Su, W., Xia, F., Chang, S. X., Brookes,
610 P. C., Dahlgren, R. A., and Xu, J.: Elevated temperature shifts soil N cycling
611 from microbial immobilization to enhanced mineralization, nitrification and
612 denitrification across global terrestrial ecosystems, *Global Change Biol.*, 26,
613 5267-5276, <https://doi.org/10.1111/gcb.15211>, 2020.
- 614 DeLuca, T. H., Keeney, D. R., and McCarty, G. W.: Effect of freeze-thaw events on
615 mineralization of soil nitrogen, *Biol. Fertil. Soils*, 14, 116-120,
616 <https://doi.org/10.1007/BF00336260>, 1992.
- 617 Deng, M., Li, P., Liu, W., Chang, P., Yang, L., Wang, Z., Wang, J., and Liu, L.:
618 Deepened snow cover increases grassland soil carbon stocks by incorporating
619 carbon inputs into deep soil layers, *Global Change Biol.*, 29, 4686-4696,
620 <https://doi.org/10.1111/gcb.16798>, 2023.
- 621 Edwards, K. A. and Jefferies, R. L.: Nitrogen uptake by *Carex aquatilis* during the
622 winter-spring transition in a low Arctic wet meadow, *J. Ecol.*, 98, 737-744,
623 <https://doi.org/10.1111/j.1365-2745.2010.01675.x>, 2010.
- 624 Elrys, A. S., Wang, J., Metwally, M. A. S., Cheng, Y., Zhang, J., Cai, Z., Chang, S. X.,
625 and Müller, C.: Global gross nitrification rates are dominantly driven by soil
626 carbon-to-nitrogen stoichiometry and total nitrogen, *Global Change Biol.*, 27,
627 6512-6524, <https://doi.org/10.1111/gcb.15883>, 2021.
- 628 Fitzhugh, R. D., Driscoll, C. T., Tierney, G. L., Fahey, T. J., and Hardy, J. P.: Effects of
629 soil freezing disturbance on soil solution nitrogen, phosphorus, and carbon
630 chemistry in a northern hardwood ecosystem, *Biogeochemistry*, 56, 215-238,
631 <https://doi.org/10.1023/A:1013076609950>, 2001.
- 632 Gao, D., Zhang, L., Liu, J., Peng, B., Fan, Z., Dai, W., Jiang, P., and Bai, E.:



- 633 Responses of terrestrial nitrogen pools and dynamics to different patterns of
634 freeze-thaw cycle: A meta-analysis, *Global Change Biol.*, 24, 2377-2389,
635 <https://doi.org/10.1111/gcb.14010>, 2018.
- 636 Hosokawa, N., Isobe, K., Urakawa, R., Tateno, R., Fukuzawa, K., Watanabe, T., and
637 Shibata, H.: Soil freeze-thaw with root litter alters N transformations during
638 the dormant season in soils under two temperate forests in northern Japan, *Soil*
639 *Biol. and Biochem.*, 114, 270-278,
640 <https://doi.org/10.1016/j.soilbio.2017.07.025>, 2017.
- 641 Han, C., Gu, Y., Kong, M., Hu, L., Jia, Y., Li, F., Sun, G., and Siddique, K.H.
642 Responses of soil microorganisms, carbon and nitrogen to freeze thaw cycles
643 in diverse land-use types, *Appl. Soil Ecol.*, 124, 211-217,
644 <https://doi.org/10.1016/j.apsoil.2017.11.012>, 2018.
- 645 IPCC (Intergovernmental Panel On Climate Change): Climate Change 2021-The
646 Physical Science Basis: Working Group I Contribution to the Sixth
647 Assessment Report of the Intergovernmental Panel on Climate Change, 1st ed.,
648 Cambridge University Press, <https://doi.org/10.1017/9781009157896>, 2023.
- 649 Ji, X., Xu, Y., Liu, H., Cai, T., and Feng, F.: Response of soil microbial diversity and
650 functionality to snow removal in a cool-temperate forest, *Soil Biol. Biochem.*,
651 196, 109515, <https://doi.org/10.1016/j.soilbio.2024.109515>, 2024.
- 652 Kaiser, C., Fuchslueger, L., Koranda, M., Gorfer, M., Stange, C. F., Kitzler, B.,
653 Rasche, F., Strauss, J., Sessitsch, A., Zechmeister-Boltenstern, S., and Richter,
654 A.: Plants control the seasonal dynamics of microbial N cycling in a beech
655 forest soil by belowground C allocation, *Ecol.*, 92, 1036-1051, 2011.
- 656 Koponen, H. T., Jaakkola, T., Keinänen-Toivola, M. M., Kaipainen, S., Tuomainen, J.,
657 Servomaa, K., and Martikainen, P. J.: Microbial communities, biomass, and
658 activities in soils as affected by freeze thaw cycles, *Soil Biol. Biochem.*, 38,
659 1861-1871, <https://doi.org/10.1016/j.soilbio.2005.12.010>, 2006.
- 660 Kreyling, J., Jurasinski, G., Grant, K., Retzer, V., Jentsch, A., and Beierkuhnlein, C.:
661 Winter warming pulses affect the development of planted temperate grassland
662 and dwarf-shrub heath communities, *Plant Ecol. Divers.*, 4, 13-21,
663 <https://doi.org/10.1080/17550874.2011.558125>, 2011.
- 664 Larsen, K. S., Michelsen, A., Jonasson, S., Beier, C., and Grogan, P.: Nitrogen Uptake
665 During Fall, Winter and Spring Differs Among Plant Functional Groups in a
666 Subarctic Heath Ecosystem, *Ecosyst.*, 15, 927-939,
667 <https://doi.org/10.1007/s10021-012-9555-x>, 2012.
- 668 Lipson, D. A., Schmidt, S. K., and Monson, R. K.: Carbon availability and
669 temperature control the post-snowmelt decline in alpine soil microbial
670 biomass, *Soil Biol. Biochem.*, 32, 441-448,
671 [https://doi.org/10.1016/S0038-0717\(99\)00068-1](https://doi.org/10.1016/S0038-0717(99)00068-1), 2000.
- 672 Lonati, M., Probo, M., Gorlier, A., and Lombardi, G.: Nitrogen fixation assessment in
673 a legume-dominant alpine community: comparison of different reference
674 species using the ^{15}N isotope dilution technique, *Alp. Bot.*, 125, 51-58,
675 <https://doi.org/10.1007/s00035-014-0143-x>, 2015.
- 676 Ma, L., Liu, G., Xu, X., Xin, X., Bai, W., Zhang, L., Chen, S., and Wang, R.: Nitrogen



- 677 acquisition strategies during the winter-spring transitional period are divergent
678 at the species level yet convergent at the ecosystem level in temperate
679 grasslands, *Soil Biol. Biochem.*, 122, 150-159,
680 <https://doi.org/10.1016/j.soilbio.2018.04.020>, 2018.
- 681 Ma, L., Zhang, C., Feng, J., Liu, G., Xu, X., Lü, Y., He, W., and Wang, R.: Retention
682 of early-spring nitrogen in temperate grasslands: The dynamics of ammonium
683 and nitrate nitrogen differ, *Glob. Ecol. and Conserv.*, 24, e01335,
684 <https://doi.org/10.1016/j.gecco.2020.e01335>, 2020.
- 685 Miller, A. E., Schimel, J. P., Sickman, J. O., Meixner, T., Doyle, A. P., and Melack, J.
686 M.: Mineralization responses at near-zero temperatures in three alpine soils,
687 *Biogeochemistry*, 84, 233-245, <https://doi.org/10.1007/s10533-007-9112-4>,
688 2007.
- 689 Miller, A. E., Schimel, J. P., Sickman, J. O., Skeen, K., Meixner, T., and Melack, J. M.:
690 Seasonal variation in nitrogen uptake and turnover in two high-elevation soils:
691 mineralization responses are site-dependent, *Biogeochemistry*, 93, 253-270,
692 <https://doi.org/10.1007/s10533-009-9301-4>, 2009.
- 693 Nie, S., Jia, X., Zou, Y., and Bian, J.: Effects of Freeze-Thaw Cycles on Soil Nitrogen
694 Transformation in Improved Saline Soils from an Irrigated Area in Northeast
695 China, *Water*, 16, 653, <https://doi.org/10.3390/w16050653>, 2024.
- 696 Nielsen, C. B., Groffman, P. M., Hamburg, S. P., Driscoll, C. T., Fahey, T. J., and
697 Hardy, J. P.: Freezing Effects on Carbon and Nitrogen Cycling in Northern
698 Hardwood Forest Soils, *Soil Sci. Soc. Am. J.*, 65, 1723-1730,
699 <https://doi.org/10.2136/sssaj2001.1723>, 2001.
- 700 Raison, R. J., Connell, M. J., and Khanna, P. K.: Methodology for studying fluxes of
701 soil mineral-N in situ, *Soil Biol. Biochem.*, 19, 521-530,
702 [https://doi.org/10.1016/0038-0717\(87\)90094-0](https://doi.org/10.1016/0038-0717(87)90094-0), 1987.
- 703 Reinmann, A. B., Susser, J. R., Demaria, E. M. C., and Templer, P. H.: Declines in
704 northern forest tree growth following snowpack decline and soil freezing,
705 *Global Change Biol.*, 25, 420-430, <https://doi.org/10.1111/gcb.14420>, 2019.
- 706 Sawicka, J. E., Robador, A., Hubert, C., Jørgensen, B. B., and Brüchert, V.: Effects of
707 freeze-thaw cycles on anaerobic microbial processes in an Arctic intertidal
708 mud flat, *ISME J.*, 4, 585-594, <https://doi.org/10.1038/ismej.2009.140>, 2010.
- 709 Schimel, J. P. and Bennett, J.: Nitrogen mineralization: Challenges of a changing
710 Paradigm, *Ecology*, 85, 591-602. <https://doi.org/10.1890/03-8002>, 2004.
- 711 Schmidt, S. K. and Lipson, D. A.: Microbial growth under the snow: Implications for
712 nutrient and allelochemical availability in temperate soils, *Plant Soil*, 259, 1-7,
713 <https://doi.org/10.1023/B:PLSO.0000020933.32473.7e>, 2004.
- 714 Sharma, S., Szele, Z., Schilling, R., Munch, J. C., and Schlöter, M.: Influence of
715 Freeze-Thaw Stress on the Structure and Function of Microbial Communities
716 and Denitrifying Populations in Soil, *Appl. Environ. Microbiol.*, 72,
717 2148-2154, <https://doi.org/10.1128/AEM.72.3.2148-2154.2006>, 2006.
- 718 Skogland, T., Lomeland, S., and Goksoyr, J.: Respiratory burst after freezing and
719 thawing of soil: Experiments with soil bacteria, *Soil Biol. Biochem.*, 20,
720 851-856, [https://doi.org/10.1016/0038-0717\(88\)90092-2](https://doi.org/10.1016/0038-0717(88)90092-2), 1988.



- 721 Sommerfeld, R. A., Mosier, A. R., and Musselman, R. C.: CO₂, CH₄ and N₂O flux
722 through a Wyoming snowpack and implications for global budgets, *Nature*,
723 361, 140-142, <https://doi.org/10.1038/361140a0>, 1993.
- 724 Song, Y., Zou, Y., Wang, G., and Yu, X.: Altered soil carbon and nitrogen cycles due
725 to the freeze-thaw effect: A meta-analysis, *Soil Biol. Biochem.*, 109, 35-49,
726 <https://doi.org/10.1016/j.soilbio.2017.01.020>, 2017.
- 727 Stark, J. M. and Hart, S. C.: Diffusion Technique for Preparing Salt Solutions,
728 Kjeldahl Digests, and Persulfate Digests for Nitrogen-15 Analysis, *Soil Sci.*
729 *Soc.Am.J.*, 60, 1846-1855, [https://doi.org/10.2136/sssaj1996.](https://doi.org/10.2136/sssaj1996.03615995006000060033x)
730 03615995006000060033x, 1996.
- 731 Sullivan, P. F., Stokes, M. C., McMillan, C. K., and Weintraub, M. N.: Labile carbon
732 limits late winter microbial activity near Arctic treeline, *Nat. Commun.*, 11,
733 4024, <https://doi.org/10.1038/s41467-020-17790-5>, 2020.
- 734 Teepe, R. and Ludwig, B.: Variability of CO₂ and N₂O emissions during freeze-thaw
735 cycles: results of model experiments on undisturbed forest-soil cores, *J. Plant*
736 *Nutr. Soil Sci.*, 167, 153-159, <https://doi.org/10.1002/jpln.200321313>, 2004.
- 737 Turner, M. M. and Henry, H. A. L.: Interactive effects of warming and increased
738 nitrogen deposition on ¹⁵N tracer retention in a temperate old field: seasonal
739 trends, *Global Change Biol.*, 15, 2885-2893,
740 <https://doi.org/10.1111/j.1365-2486.2009.01881.x>, 2009.
- 741 Vance, E. D., Brookes, P. C., and Jenkinson, D. S.: An extraction method for
742 measuring soil microbial biomass C, *Soil Biol. Biochem.*, 19, 703-707,
743 [https://doi.org/10.1016/0038-0717\(87\)90052-6](https://doi.org/10.1016/0038-0717(87)90052-6), 1987.
- 744 Walker, D.A., Epstein, H.E., Gould, W.A., Kelley, A.M., Kade, A.N., Knudson, J.A.,
745 Krantz, W.B., Michaelson, G., Peterson, R.A., Ping, C.-L., Raynolds, M.K.,
746 Romanovsky, V.E. and Shur, Y.: Frost-boil ecosystems: complex interactions
747 between landforms, soils, vegetation and climate, *Permafr. Periglac. Process.*,
748 15, 171-188, <https://doi.org/10.1002/ppp.487>, 2004.
- 749 Walker, V. K., Palmer, G. R., and Voordouw, G.: Freeze-Thaw Tolerance and Clues to
750 the Winter Survival of a Soil Community, *Appl. Environ. Microbiol.*, 72,
751 1784-1792, <https://doi.org/10.1128/AEM.72.3.1784-1792.2006>, 2006.
- 752 Wang, A., Wu, F., Yang, W., Wu, Z., Wang, X., and Tan, B.: Abundance and
753 composition dynamics of soil ammonia-oxidizing archaea in an alpine fir
754 forest on the eastern Tibetan Plateau of China, *Can. J. Microbiol.*, 58, 572-580,
755 <https://doi.org/10.1139/w2012-032>, 2012.
- 756 Wang, Q., Chen, M., Yuan, X., and Liu, Y.: Effects of Freeze-Thaw Cycles on
757 Available Nitrogen Content in Soils of Different Crops, *Water*, 16, 2348,
758 <https://doi.org/10.3390/w16162348>, 2024.
- 759 Wang, R., Tian, Y., Ouyang, S., Xu, X., Xu, F., and Zhang, Y.: Nitrogen acquisition
760 strategies used by *Leymus chinensis* and *Stipa grandis* in temperate steppes,
761 *Biol. Fertil. Soils*, 52, 951-961, <https://doi.org/10.1007/s00374-016-1128-2>,
762 2016.
- 763 Yanai, Y., Toyota, K., and Okazaki, M.: Response of denitrifying communities to
764 successive soil freeze-thaw cycles, *Biol. Fertil. Soils*, 44, 113-119,



- 765 <https://doi.org/10.1007/s00374-007-0185-y>, 2007.
- 766 Yang, X., Hou, R., Fu, Q., Li, T., Wang, J., Su, Z., Shen, W., Zhou, W., and Wang, Y.:
767 Effect of freeze-thaw cycles and biochar coupling on the soil water-soil
768 environment, nitrogen adsorption and N₂O emissions in seasonally frozen
769 regions, *Sci. Total Environ.*, 893, 164845,
770 <https://doi.org/10.1016/j.scitotenv.2023.164845>, 2023.
- 771 Ye, Y., Wang, W., Zheng, C., Fu, D. and Liu, H. : Evaluation of cold resistance of four
772 wild *Carex* species. *Chin. J. Appl. Ecol.*, 28, 89-95, 2017.
- 773 Yu, X., Zou, Y., Jiang, M., Lu, X., and Wang, G.: Response of soil constituents to
774 freeze-thaw cycles in wetland soil solution, *Soil Biol. Biochem.*, 43,
775 1308-1320, <https://doi.org/10.1016/j.soilbio.2011.03.002>, 2011.
- 776 Zhang, X., Bai, W., Gilliam, F. S., Wang, Q., Han, X., and Li, L.: Effects of in situ
777 freezing on soil net nitrogen mineralization and net nitrification in fertilized
778 grassland of northern China, *Grass Forage Sci.*, 66, 391-401,
779 <https://doi.org/10.1111/j.1365-2494.2011.00789.x>, 2011.
- 780 Zhang, Y., Hou, R., Fu, Q., Li, T., Li, M., Dong, S., and Shi, G.: Soil environment,
781 carbon and nitrogen cycle functional genes in response to freeze-thaw cycles
782 and biochar, *J. Cleaner Prod.*, 444, 141345,
783 <https://doi.org/10.1016/j.jclepro.2024.141345>, 2024.
- 784 Zheng, Z., Qu, Z., Diao, Z., Zhang, Y., and Ma, L.: Efficient utilization of winter
785 nitrogen sources by soil microorganisms and plants in a temperate grassland,
786 *Glob. Ecol. Conserv.*, 54, e03135, <https://doi.org/10.1016/j.gecco.2024.e03135>,
787 2024.
- 788 Zhou, J., Chen, Z., and Li, S.: Oxidation Efficiency of Different Oxidants of
789 Persulfate Method Used to Determine Total Nitrogen and Phosphorus in
790 Solutions, *Commun. Soil Sci. Plant Anal.*, 34, 725-734,
791 <https://doi.org/10.1081/CSS-120018971>, 2003.
- 792 Zong N. and Shi P.: Effects of winter warming on carbon and nitrogen cycling in
793 alpine ecosystems: a review, *Acta Ecol. Sinica*, 40, 3131-3143,
794 <https://doi.org/10.5846/stxb201904040655>, 2020.



795 **Table 1** Climate, soil, and plant community properties (\pm Standard Error) in the meadow steppe
796 and the sandy steppe (n = 6).

	Term	Meadow steppe	Sandy steppe
Site information	Location	49°19' N, 120°02' E	39°29' N, 110°11' E
	Soil type	Loam soil	Sandy loam soil
	MAT (°C)	-1.5~1	6.5
	MAP (mm)	420	310
	Elevation (m)	628	1290
	Frequency of spring freeze-thaw cycle (times)	19	21
Soil property	STC (kg m ⁻²)	3.98 \pm 0.14*	1.00 \pm 0.10
	SIN (g m ⁻²)	1.79 \pm 0.09*	0.86 \pm 0.05
	20-2000 μ m (%)	63.71 \pm 1.58*	48.59 \pm 1.98
	2-20 μ m (%)	27.23.13 \pm 0.63*	36.74 \pm 0.67
	< 2 μ m (%)	10.13 \pm 0.23*	6.42 \pm 0.13
	pH	7.36 \pm 0.26	8.57 \pm 0.07
	BD	1.37 \pm 0.11	1.26 \pm 0.10
Plant property	Cover (%)	<i>Stipa baicalensis</i>	<i>Hedysarum mongolicum</i> 40 \pm 1.26
		<i>Leymus chinensis</i>	<i>Cleistogenes squarrosa</i> 20 \pm 0.86
		<i>Carex pediformis</i>	<i>Klasea centauroides</i> 25 \pm 0.59
			12 \pm 0.48
The treatment times	HFTC	7 March, 9 March, 10 March, 12 March, 14 March, 15 March, 17 March, 18 March, 20 March, 21 March, 23 March, and 26 March 2021	10 February, 16 February, 18 February, 20 February, 21 February, 23 February, 25 February, 26 February, 28 February, 1 March, 3 March, and 5 March 2021
	LFTC	7 March, 10 March, 14 March, 17 March, 20 March, and 23 March 2021	10 February, 18 February, 21 February, 25 February, 28 February, and 3 March 2021

Significant differences between sites were identified using One-way ANOVAs: *, $p < 0.05$. MAT, mean annual temperature; MAP, mean annual precipitation; STC, soil total C content; SIN, soil inorganic N content; BD, soil bulk density; HFTC, increased high frequency freeze-thaw cycles (12 times); LFTC, increased low frequency freeze-thaw cycles (6 times).



Figure Legends

Figure 1. Geographical distribution of the transect in a meadow steppe and a sandy steppe in northern China.

Figure 2. Soil temperature (Figure. 2a) and moisture (Figure. 2b) from autumn 2020 to autumn 2021 under intensified low-frequency freeze-thaw cycles (LFTC; 6 times) and high-frequency freeze-thaw cycles (HFTC; 12 times) treatments in a meadow steppe and a sandy steppe in northern China. Shaded vertical bars indicate processing (treatment) period. Vertical lines indicate natural freeze-thaw periods. Nabras indicate sampling times, dates for ^{15}N tracer injection and sampling dates are also shown.

Figure 3. Soil $\text{NH}_4^+\text{-N}$, $\text{NO}_3^-\text{-N}$, net ammoniation and net nitrification rates under intensified low-frequency freeze-thaw cycles (LFTC; 6 times) and high-frequency freeze-thaw cycles (HFTC; 12 times) treatments in a meadow steppe and a sandy steppe in northern China. Vertical bars indicate the standard error (SE) of the means ($n = 6$). Different lowercase letters indicate statistically significant differences among treatment groups within sampling periods ($p < 0.05$).

Figure 4. Soil microbial biomass C and N under intensified low-frequency freeze-thaw cycles (LFTC; 6 times) and high-frequency freeze-thaw cycles (HFTC; 12 times) treatments in a meadow steppe and a sandy steppe in northern China. Vertical bars indicate the standard error (SE) of the means ($n = 6$). Different lowercase letters indicate statistically significant differences among sampling periods ($p < 0.05$).

Figure 5. Plant biomass N (shoot and root) under intensified low-frequency freeze-thaw cycles (LFTC; 6 times) and high-frequency freeze-thaw cycles (HFTC; 12 times) treatments in a meadow steppe and a sandy steppe in northern China. Vertical bars indicate the SE of the means ($n = 6$). Different lowercase letters indicate statistically significant differences among sampling periods ($p < 0.05$).

Figure 6. Dynamics of ^{15}N tracers in soils, microorganisms, and plants under intensified



low-frequency freeze-thaw cycles (LFTC; 6 times) and high-frequency freeze-thaw cycles (HFTC; 12 times) treatments in a meadow steppe and a sandy steppe in northern China.

Vertical bars indicate the SE of the means ($n = 6$). Different lowercase letters indicate statistically significant differences among sampling periods ($p < 0.05$).

Figure 7. Plant ^{15}N acquisition under intensified low-frequency freeze-thaw cycles (LFTC; 6 times) and high-frequency freeze-thaw cycles (HFTC; 12 times) treatments in a meadow steppe and a sandy steppe. Vertical bars indicate the SE of the mean ($n = 6$). Different lowercase letters indicate statistically significant differences among sampling periods ($p < 0.05$).

Figure 8. Relationships between plant ^{15}N acquisition and environmental predictors under intensified low freeze-thaw cycle (LFTC; 6 times) and high freeze-thaw cycle (HFTC; 12 times) treatments in the meadow steppe and the sandy steppe. DOC represents dissolved organic C content, DON represents dissolved organic N content, F:B denotes the fungal to bacterial biomass ratio, and MBC:MBN indicates the microbial biomass C to N ratio.

Figure 9. Relative importance of environmental predictors for plant ^{15}N acquisition as determined by random forest analysis under intensified low freeze-thaw cycle (LFTC; 6 times) and high freeze-thaw cycle (HFTC; 12 times) treatments in the meadow steppe and the sandy steppe. Predictor importance is expressed as percentage increase in mean squared error (%IncMSE) when each variable is permuted. DOC represents dissolved organic C content, DON represents dissolved organic N content, F:B denotes the fungal to bacterial biomass ratio, and MBC:MBN indicates the microbial biomass C to N ratio.

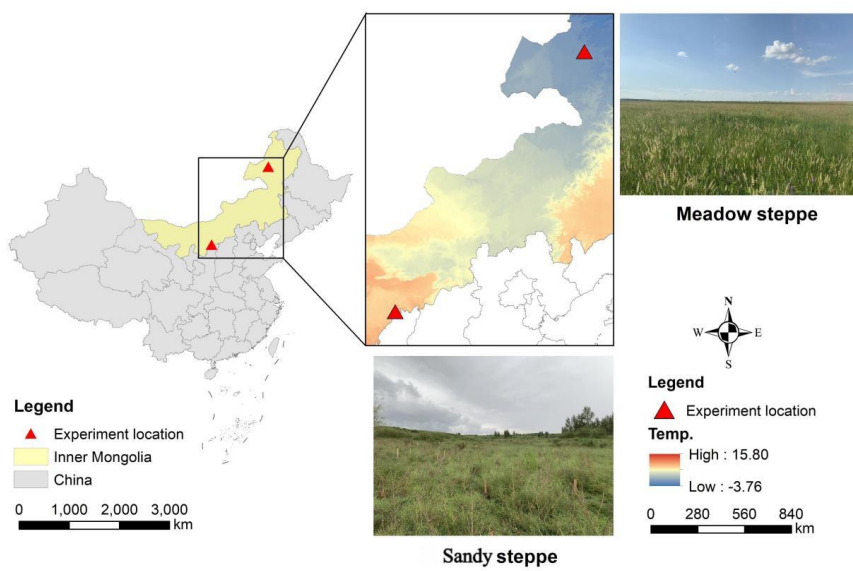


Figure 1. Geographical distribution of the transect in a meadow steppe and a sandy steppe in northern China.

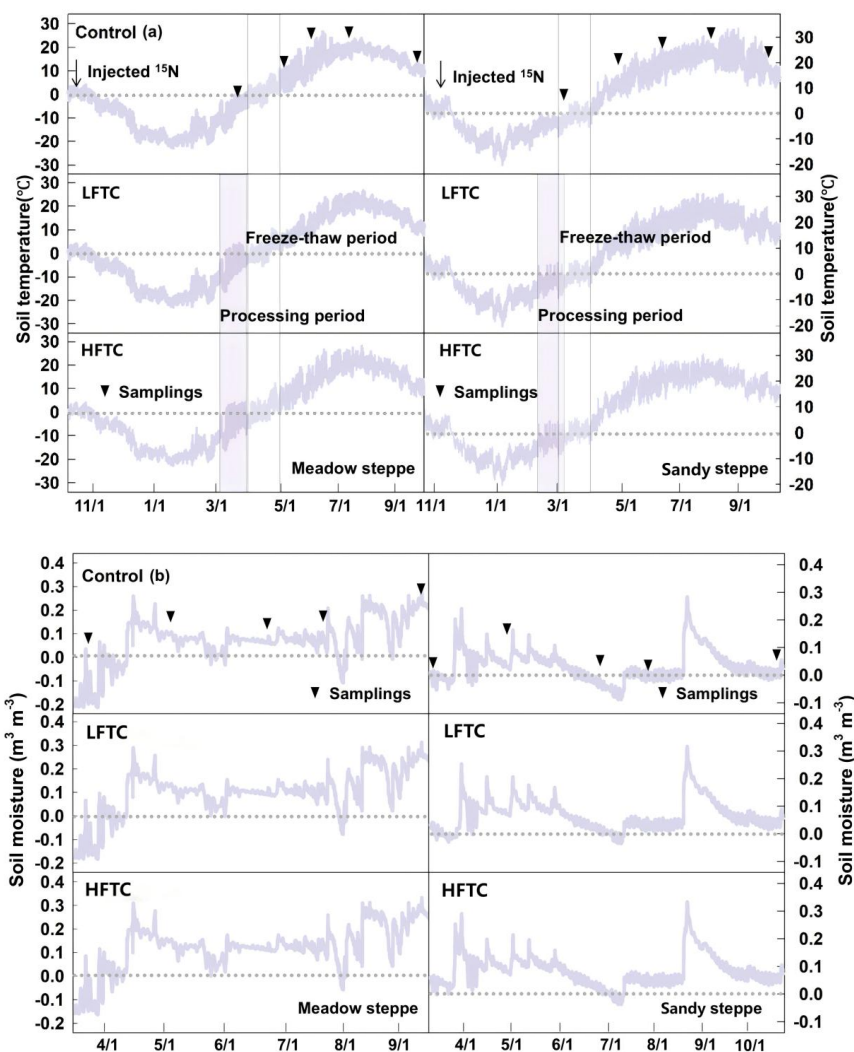


Figure 2. Soil temperature (Figure. 2a) and moisture (Figure. 2b) from autumn 2020 to autumn 2021 under intensified low-frequency freeze-thaw cycles (LF; 6 times) and high-frequency freeze-thaw cycles (HF; 12 times) treatments in a meadow steppe and a sandy steppe in northern China. Shaded vertical bars indicate processing (treatment) period. Vertical lines indicate natural freeze-thaw periods. Nabras indicate sampling times, dates for ¹⁵N tracer injection and sampling dates are also shown.

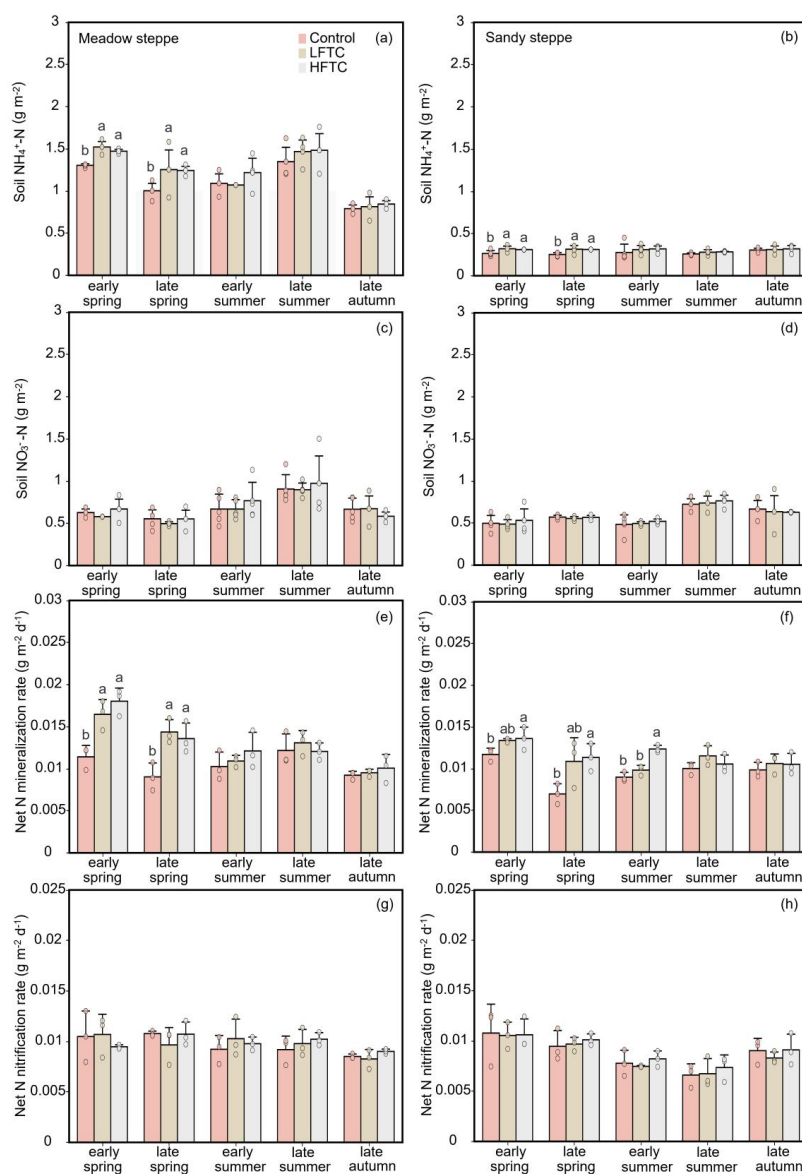


Figure 3. Soil $\text{NH}_4^+\text{-N}$, $\text{NO}_3^-\text{-N}$, net ammoniation and net nitrification rates under intensified low-frequency freeze-thaw cycles (LFTC; 6 times) and high-frequency freeze-thaw cycles (HFTC; 12 times) treatments in a meadow steppe and a sandy steppe in northern China. Vertical bars indicate the standard error (SE) of the means ($n = 6$). Different lowercase letters indicate statistically significant differences among treatment groups within sampling periods ($p < 0.05$).

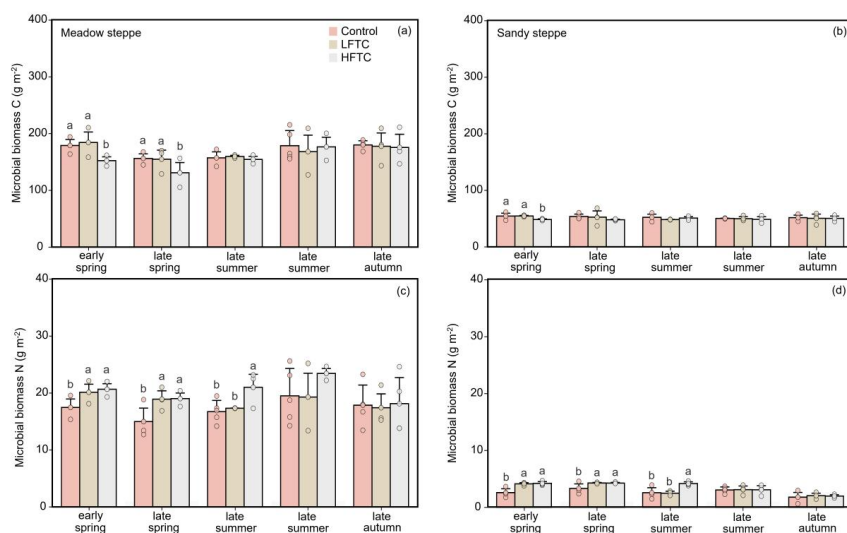


Figure 4. Soil microbial biomass C and N under intensified low-frequency freeze-thaw cycles (LFTC; 6 times) and high-frequency freeze-thaw cycles (HFTC; 12 times) treatments in a meadow steppe and a sandy steppe in northern China. Vertical bars indicate the standard error (SE) of the means (n = 6). Different lowercase letters indicate statistically significant differences among sampling periods ($p < 0.05$).

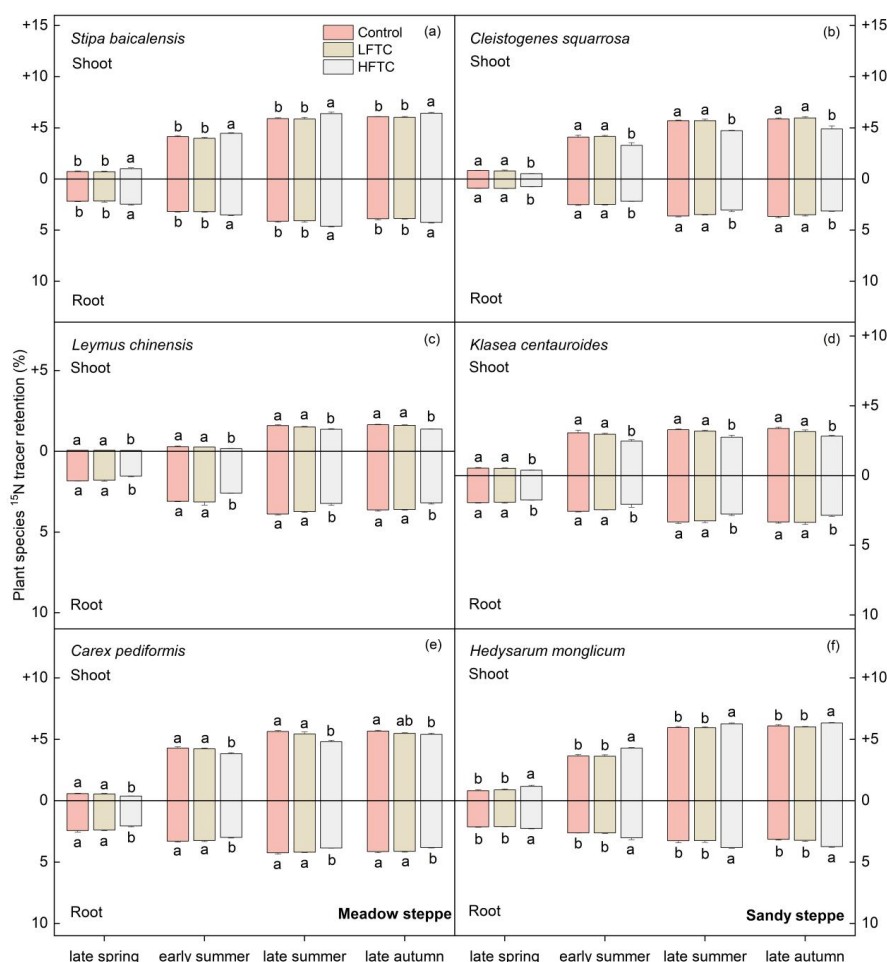


Figure 5. Plant biomass N (shoot and root) under intensified low-frequency freeze-thaw cycles (LFTC; 6 times) and high-frequency freeze-thaw cycles (HFTC; 12 times) treatments in a meadow steppe and a sandy steppe in northern China. Vertical bars indicate the SE of the means (n = 6). Different lowercase letters indicate statistically significant differences among sampling periods (p < 0.05).

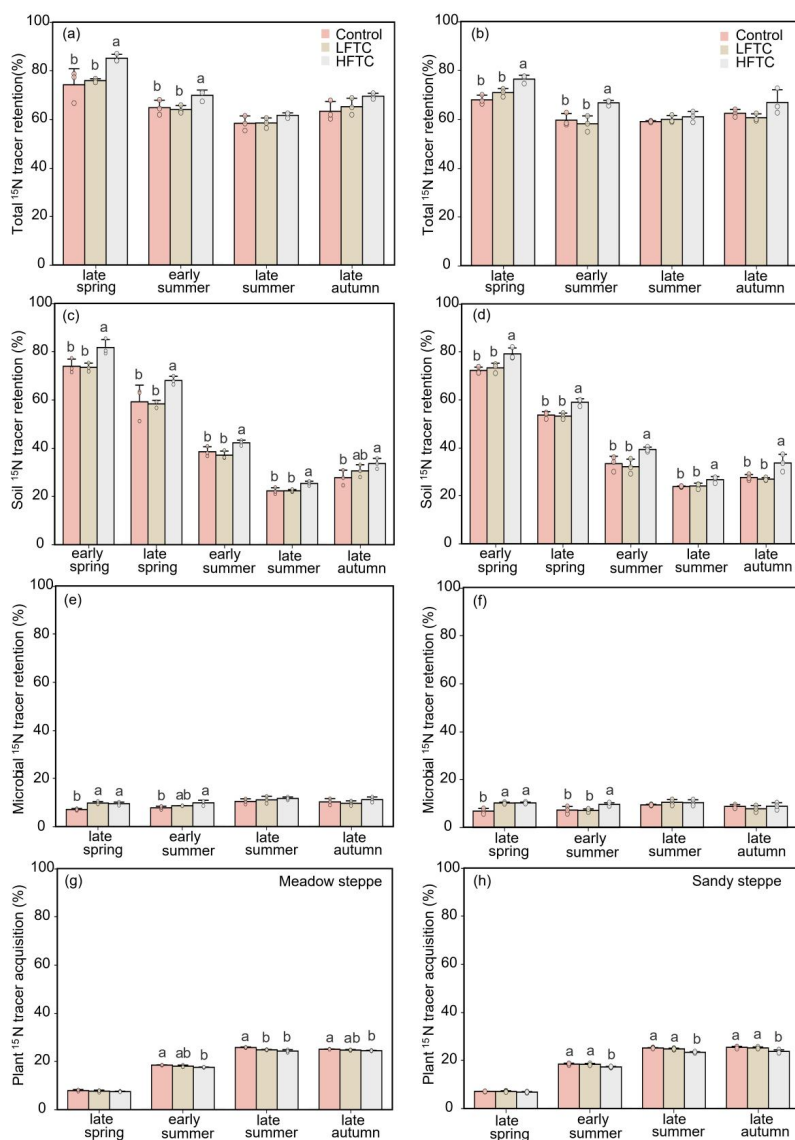


Figure 6. Dynamics of ^{15}N tracers in soils, microorganisms, and plants under intensified low-frequency freeze-thaw cycles (LFTC; 6 times) and high-frequency freeze-thaw cycles (HFTC; 12 times) treatments in a meadow steppe and a sandy steppe in northern China. Vertical bars indicate the SE of the means ($n = 6$). Different lowercase letters indicate statistically significant differences among sampling periods ($p < 0.05$).

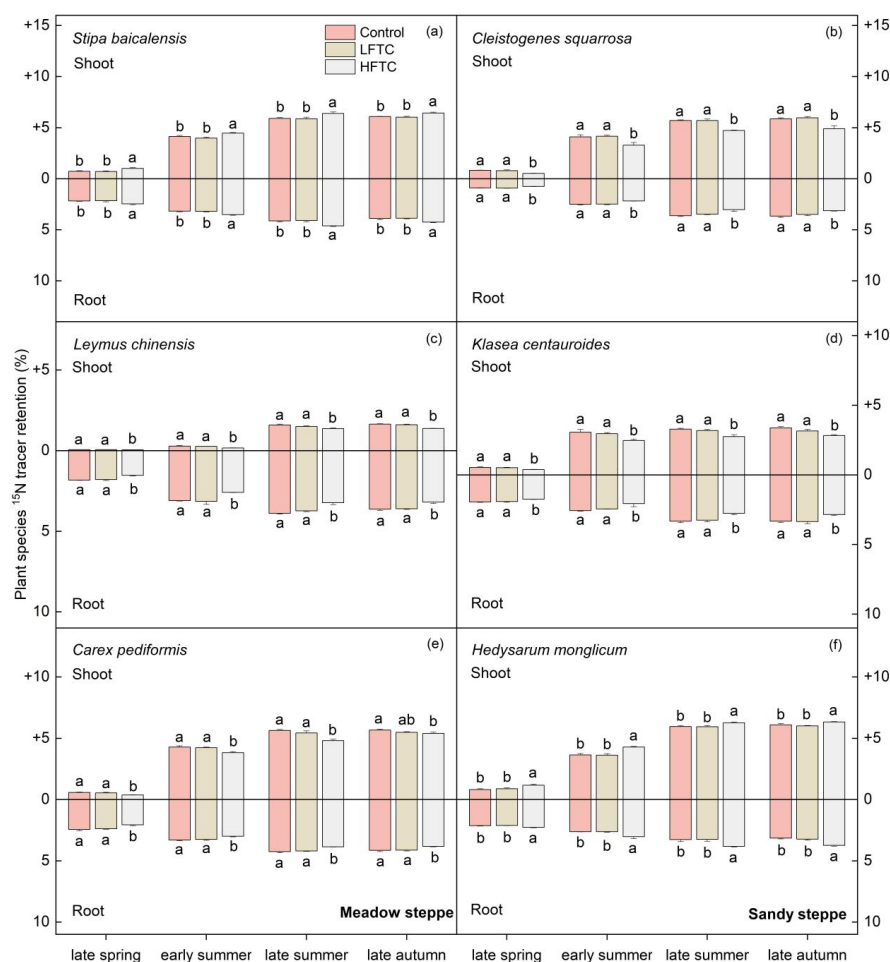


Figure 7. Plant ^{15}N acquisition under intensified low-frequency freeze-thaw cycles (LFTC; 6 times) and high-frequency freeze-thaw cycles (HFTC; 12 times) treatments in a meadow steppe and a sandy steppe. Vertical bars indicate the SE of the mean ($n = 6$). Different lowercase letters indicate statistically significant differences among sampling periods ($p < 0.05$).

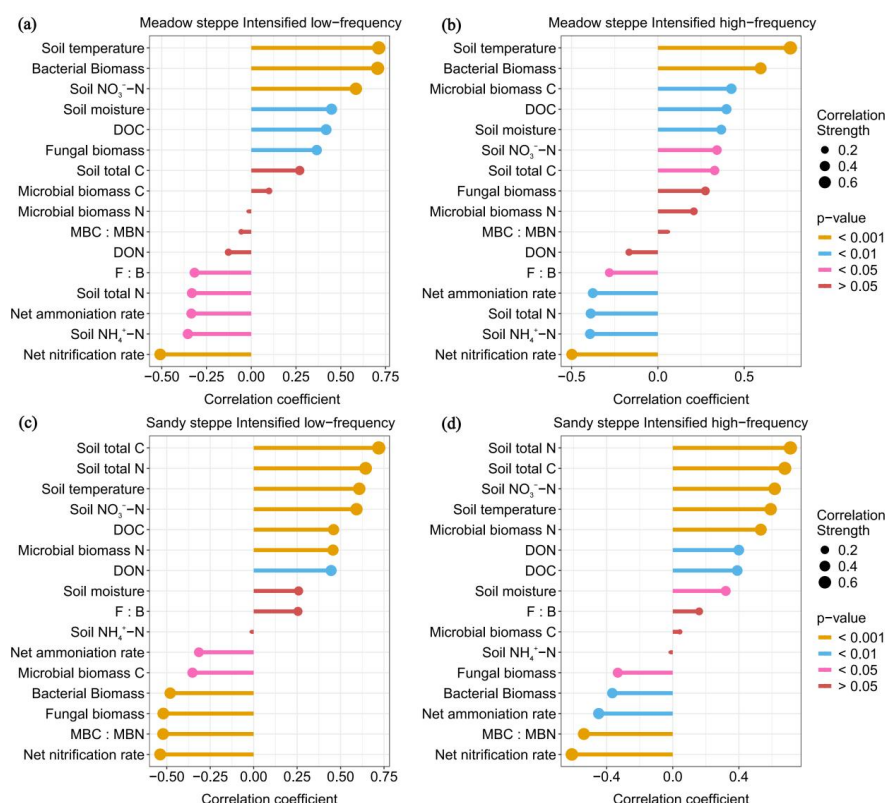


Figure 8. Relationships between plant ¹⁵N acquisition and environmental predictors under intensified low freeze-thaw cycle (LFTC; 6 times) and high freeze-thaw cycle (HFTC; 12 times) treatments in the meadow steppe and the sandy steppe. DOC represents dissolved organic C content, DON represents dissolved organic N content, F:B denotes the fungal to bacterial biomass ratio, and MBC:MBN indicates the microbial biomass C to N ratio.

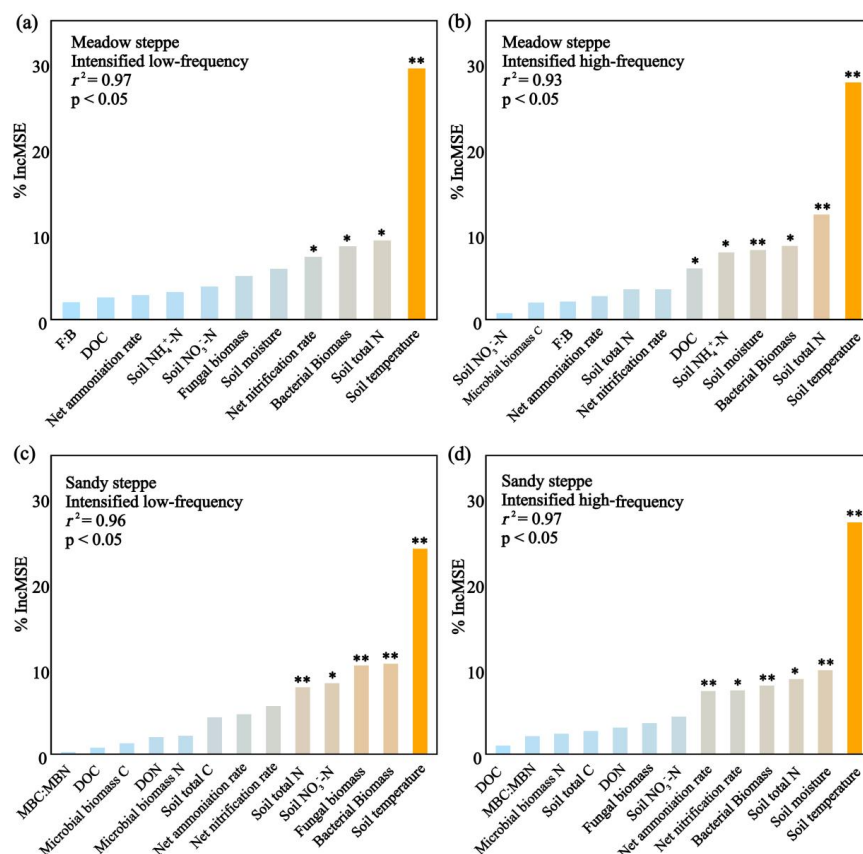


Figure 9. Relative importance of environmental predictors for plant ^{15}N acquisition as determined by random forest analysis under intensified low freeze-thaw cycle (LFTC; 6 times) and high freeze-thaw cycle (HFTC; 12 times) treatments in the meadow steppe and the sandy steppe. Predictor importance is expressed as percentage increase in mean squared error (%IncMSE) when each variable is permuted. DOC represents dissolved organic C content, DON represents dissolved organic N content, F:B denotes the fungal to bacterial biomass ratio, and MBC:MBN indicates the microbial biomass C to N ratio.